LABORATÓRIO DE INSTRUMENTAÇÃO E
FÍSICA EXPERIMENTAL DE PARTÍCULAS

LIP / 95–02
February 1995

The evolution of cross section ratio $\psi'/J/\psi$ from p-A to S-U interactions. Direct photon emission in correlation with ϕ and J/ψ

Sérgio Ramos[1)]

LIP Lisbon
and
IST, Universidade Técnica de Lisboa

NA38 Collaboration

Abstract

J/ψ and ψ' production cross sections are studied for several proton induced reactions and in S-U collisions, in the NA38 experiment, by measuring the resonances' decays in the muon pair channel. Whereas in p-A interactions the $\psi'/J/\psi$ ratio remains constant going from p-p and p-d collisions to p-W and p-U ones, with a mean value of $1.76\% \pm 0.04\%$, in the S-U data it exhibits half of this value and it decreases as centrality of the collision increases. Also studied are the differences between the γ/π^0 ratio yields correlated with the J/ψ mass range and other dimuon masses: no significant effect is seen.

Talk presented at Quark Matter '95
Monterey, California, USA, 9-13 January 1995

[1]LIP, Av. Elias Garcia 14, P-1000 Lisboa, Portugal (e-mail: siocha@vaxlip.lip.pt)

The evolution of cross section ratio $\psi'/J/\psi$ from p-A to S-U interactions. Direct photon emission in correlation with ϕ and J/ψ

Presented by Sérgio Ramos[4b]

NA38 Collaboration

M.C. Abreu[4a], C. Baglin[1], A. Baldit[2], C. Barrière[2], M. Bedjidian[9], P. Bordalo[4b], A. Borhani[6], A. Bussière[1], J. Castor[2], T. Chambon[2], B. Chaurand[6], D. Contardo[9], E. Descroix[9], A. Devaux[2], O. Drapier[9], B. Espagnon[2], J. Fargeix[2], F. Fleuret[6], P. Force[2], J. Gago[4b], C. Gerschel[5], M. Gonin[6], P. Gorodetzky[7], J.Y. Grossiord[9], A. Guichard[9], J.P. Guillaud[1], R. Haroutunian[9], D. Jouan[5], L. Kluberg[6], R. Kossakowski[1], G. Landaud[2], C. Lourenço[4♯], L. Luquin[2], F. Malek[8], R. Mandry[8], R. Mazini[7], J.R. Pizzi[9], C. Racca[7], S. Ramos[4b], A. Romana[6], B. Ronceux[1], S. Silva[4], P. Sonderegger[3b], X. Tarrago[5], J. Varela[4b♯]

[1] Laboratoire d'Annecy-le-Vieux de Physique des Particules, IN2P3-CNRS, B.P. 110, F-74941 Annecy-le-Vieux Cedex, France

[2] Laboratoire de Physique Corpusculaire de Clermont-Ferrand, IN2P3-CNRS et Université Blaise Pascal, F-63177 Aubière Cedex, France

[3] CERN, CH-1211 Geneva 23, Switzerland

[4] LIP, Av. Elias Garcia 14, P-1000 Lisbon, Portugal

[5] Institut de Physique Nucléaire, IN2P3-CNRS et Université de Paris-Sud, F-91406 Orsay Cedex, France

[6] Laboratoire de Physique Nucléaire des Hautes Energies, Ecole Polytechnique, IN2P3-CNRS, F-91128 Palaiseau Cedex, France

[7] Centre de Recherches Nucléaires, IN2P3-CNRS et Université Louis Pasteur, BP 20, F-67037 Strasbourg Cedex, France

[9] Institut de Physique Nucléaire de Lyon, IN2P3-CNRS et Université Claude Bernard, 43 Boulevard du 11 Novembre 1918, F-69622 Villeurbanne Cedex, France

[a] Also at FCUL, Universidade de Lisboa, Lisbon, Portugal.

[b] Also at IST, Universidade Técnica de Lisboa, Lisbon, Portugal.

♯Present address CERN Geneva, Switzerland.

J/ψ and ψ' production cross sections are studied for several proton induced reactions and in S-U collisions, in the NA38 experiment, by measuring the resonances' decays in the muon pair channel. Whereas in p-A interactions the $\psi'/J/\psi$ ratio remains constant going from p-p and p-d collisions to p-W and p-U ones, with a mean value of $1.76\% \pm 0.0$[illegible], in the S-U data it exhibits half of this value and it decreases as centrality of the collision increases. Also studied are the differences between the γ/π^o ratio yields correlated with the J/ψ mass range and other dimuon masses; no significant effect is seen.

1. INTRODUCTION

The NA38 experiment uses the SPS accelerator at CERN and detects muons produced in p-A and S-U collisions at different energies. It triggers on muon pairs and is also able to measure neutral transverse energy, E_T^a, and charged particle multiplicities, n_{ch}, correlated with the dimuon mass, $M_{\mu\mu}$.

As NA38 deals with high intensity beams, ψ' statistics could be accumulated for different p-A systems and for S-U interactions.

The motivation of such a study relies on the different theoretical predictions concerning the ψ' behaviour in the Quark-Gluon Plasma (QGP) framework and in hadronic rescattering models [1]. Our first aim in this report is to study the ψ' evolution, as compared to J/ψ, from p-A to S-U collisions.

On the other hand, NA38 has also measured J/ψ suppression [2] and ϕ enhancement [3] in S-U interactions at 200 GeV/nucleon. These observations are in agreement with standard QGP predictions. Such predictions imply, for central collisions, that J/ψ channel emphasizes non-plasma events, as it survives better in a non-QGP environment; and that ϕ channel favours events with QGP formation, as chemical equilibrium allows strangeness abundances to increase. In this context, we may ask if ϕ events radiate more than J/ψ ones. Our second goal is the study of direct photon emission in correlation with ϕ and J/ψ signals.

2. EXPERIMENTAL SETUPS

The NA38 detector [4] consists mainly of a muon spectrometer, an electromagnetic calorimeter which measures the neutral transverse energy released in the interaction, and an active target formed by several subtargets and a set of cylindrical scintillators surrounding them, from which we obtain the interaction point and a measure of the charged particle multiplicity.

Different layouts are used. The setup dealing with sulphur beams is described in detail elsewhere [4]. Here we focus on the proton-nucleus special configuration setups. In order to obtain reasonable statistics with different systems covering a wide mass number range: H_2, D_2, C, Al, Cu and W, proton intensities were almost an order of magnitude greater than ion ones (10^8/burst in p-A as compared to $1.8 \cdot 10^8$ in S-U). This is is only possible using SPS primary beams at 450 GeV/c.

Also, the usual 20% interaction length uranium targets, used in sulphur induced reactions, were replaced by targets having a factor of three more. Nevertheless, in some systems (p-Cu and p-W) two target thicknesses allowed us to control results' quality, namely mass resolution differences, which extend from 74 to 88 MeV at the J/ψ, and secondary interaction rates, found to be negligible.

The experimental layout for the proton induced interactions impinging on H_2 and D_2 was specially designed for other physical purposes (NA51 Collaboration - Study of the isospin symmetry breaking in the light quark sea of the nucleon from the Drell-Yan process) [5]. J/ψ and ψ' analysis is thus a by-product of our NA51 data. For these systems, due to the long targets used, J/ψ mass resolution is 175 MeV.

In p-A interactions the number of nucleon-nucleon collisions inside the target nucleus is small and thus subject to large fluctuations, whatever the impact parameter of the

reaction may be. Due to this, the neutral transverse energy E_T^o is very weakly correlated to the geometry of the interaction. As a consequence, the electromagnetic calorimeter, made of scintillating fibres embedded in lead in a 1:2 volume ratio, was replaced by a BeO absorber which, while fighting background at the same level, improves mass resolution.

3. DATA ANALYSIS

On the reconstruction of the experimental data events, selection criteria concerning track quality and chamber's fiducial volumes are applied. In view of the background subtraction, one imposes the same μ^+ and μ^- acceptances by applying an additional cut, which rejects each track whose opposite charge image track would fell out of the spectrometer's acceptance. NA38 background comes from π and K decays into muons. The background yield is deduced from the like-sign distributions in each dimuon mass bin and as a function of the magnetic field sign (which is reversed frequently) with the usual expression

$$N_{Bg}^{+-} = 2 \cdot R \cdot (\sqrt{N_+^{++} N_+^{--}} + \sqrt{N_-^{++} N_-^{--}}) \quad , \tag{1}$$

where N subscripts stand for the magnetic field signs and R is a factor depending on the collision type. For p-A interactions, R was measured with the help of two extreme setup configurations, in what concerns the amount of absorbers used. Combining these results, knowing that the dimuon signal should be the same in both, whereas the background should be less in the larger absorber setup, one obtains $R^{pA} = 1.25 \pm 0.04 \pm 0.06$, in accordance with our Fritiof based Monte-Carlo simulations. For S-U interactions, one relies on the simulation value and use $R^{SU} = 1$. In fact, the background extraction expression with $R_{\cdot} = 1$ is rigorous for independent and poissonian like-sign distributions, which is the case for S-U, with $E_T^o > 13\ GeV$, but not for p-A, where multiplicities are small.

In this way, background is subtracted from the data, prior to any comparison with our Monte-Carlo simulations.

In the dimuon mass region of interest for this analysis the physical ingredients are the J/ψ and ψ' resonances, the Drell-Yan and $D\bar{D}$ distributions. As beyond $M_{\mu\mu} \geq 2.9$ GeV/c^2 $D\bar{D}$ becomes negligible, only the first three contributions are generated, using the NA38 Monte-Carlo simulation program. For Drell-Yan, GRV(HO) [6] structure functions parametrization is used, and one takes isospin into account ($\sigma_{pp}^{DY} \neq \sigma_{nn}^{DY} \neq \sigma_{pn}^{DY} \neq \sigma_{np}^{DY}$) in the σ_{SU}^{DY} generation. J/ψ and ψ' masses and widths are generated according to their nominal values.

Each kind of simulated events, that is, Drell-Yan, J/ψ and ψ', is separately reconstructed with the NA38 program used also to reconstruct real data. Analytical functions are used to smooth each kind of reconstructed events. Finally, to fit the experimental data, we use a superposition of the three component's analytical functions:

$$\frac{dN^{signal}}{dM_{\mu\mu}} = C_{J/\psi} \cdot \frac{dN^{J/\psi}}{dM_{\mu\mu}} + C_{\psi'} \cdot \frac{dN^{\psi'}}{dM_{\mu\mu}} + C_{DY} \cdot \frac{dN^{DY}}{dM_{\mu\mu}} \quad . \tag{2}$$

Figures 1 and 2 show the $N_{\mu\mu}^{signal}$ distributions, for p-Cu collisions at 450 GeV/nucleon and S-U interactions at 200 GeV/nucleon, where the generated contributions have been

superimposed. One sees that both fits are good, the χ^2/ndf being 1.62 and 1.16, respectively.

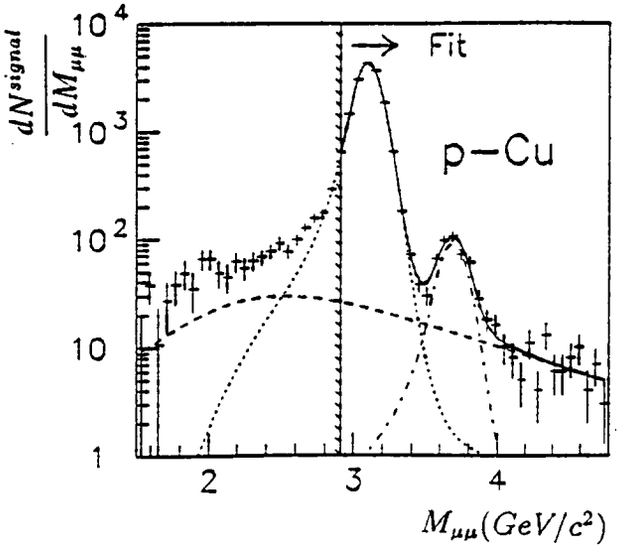

Figure 1. Signal dimuon mass distribution in p-Cu collisions.

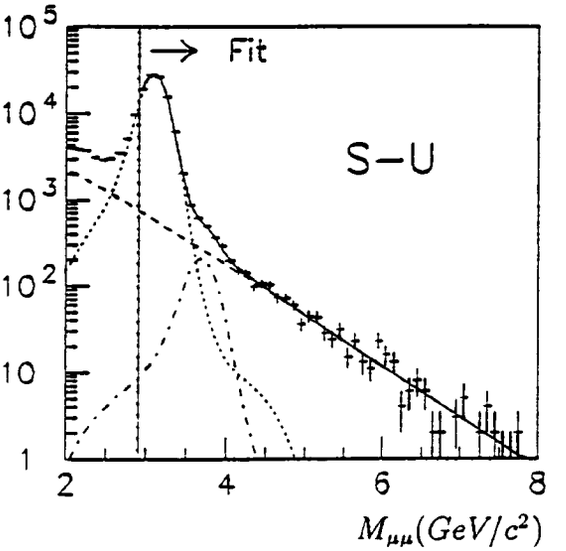

Figure 2. Signal dimuon mass distribution in S-U collisions.

4. RESULTS ON $\psi'/J/\psi$ CROSS SECTION MEASUREMENTS

4.1. Study of p-A interactions

For all p-A systems at 450 GeV/nucleon, our analysis is performed in the following kinematical domain: cms rapidity region of $-0.5 < y_{cm} < 0.7$ and scattering angle region, in the Collins-Sopper frame, of $-0.5 < cos\ \theta^* < 0.5$. Table 1 shows the number of ψ', J/ψ and signal events for $M_{\mu\mu} \geq 1.5\ GeV/c^2$, for the analysis of proton induced interactions.

Table 1
Number of events in p-A collisions

System (target length, cm)	$N_{\mu\mu}^{signal}$ $M_{\mu\mu} \geq 1.5\ GeV/c^2$	$N^{J/\psi}$	$N^{\psi'}$
$p - H_2$ (120.0)	484509	441969	10152
$p - D_2$ (120.0)	490417	454077	10802
$p - C$ (30.0)	16568	14966	399
$p - Al$ (20.0)	2135	1862	30
$p - Cu$ (10.1)	18327	16544	383
$p - Cu$ (2.0)	2318	2083	43
$p - W$ (5.6)	13082	11579	247
$p - W$ (1.5)	2202	1907	49

In order to extract cross sections, ψ' and J/ψ are corrected for acceptance. The analysis of $\psi'/J/\psi$ cross section ratio in the $\mu\mu$ channel ($B_{\psi'}\sigma_{\psi'}/B_{J/\psi}\sigma_{J/\psi}$) is performed as a function of the target mass number A and of the particle mean path in the target nucleus L. L is calculated within a geometrical model [7].

To compare our results at 450 GeV/c with our previous ones, p-W and p-U data at 200 GeV/nucleon, which were presented at QM'93 [8], we perform the energy rescaling of the ratio $B_{\psi'}\sigma_{\psi'}/B_{J/\psi}\sigma_{J/\psi}$. For this, we use the so-called Craigie parametrization $\sigma_i = C_i \cdot exp(-14.7\ M_i/\sqrt{s})$, where $i \equiv \psi', J/\psi, \chi$ and we take into account ψ' and both χ decays into J/ψ:

$$\sigma_{J/\psi}(\sqrt{s}) = \sigma_{\psi_{dir}}(\sqrt{s}) + \sigma_{\psi'\to\psi}(\sqrt{s}) + \sigma_{\chi\to\psi}(\sqrt{s}) \quad .$$

That is, values of the ratio at energy $\sqrt{s_2}$ are obtained from those at energy $\sqrt{s_1}$ using

$$\left(\frac{B_{\psi'}\sigma_{\psi'}}{B_{J/\psi}\sigma_{J/\psi}}\right)_{\sqrt{s_2}} = \frac{\sigma_{\psi'}(\sqrt{s_2})/\sigma_{J/\psi}(\sqrt{s_2})}{\sigma_{\psi'}(\sqrt{s_1})/\sigma_{J/\psi}(\sqrt{s_1})} \cdot \left(\frac{B_{\psi'}\sigma_{\psi'}}{B_{J/\psi}\sigma_{J/\psi}}\right)_{\sqrt{s_1}} \quad .$$

Table 2 shows such rescaling applied to our data. As corrections are small, of the order of 10%, the question concerning the quality of the used parametrization is not important. Also shown are four other experiment's values [9].

Table 2
Rescaling of the ratio $B_{\psi'}\sigma_{\psi'}/B_{J/\psi}\sigma_{J/\psi}$ from 450 to 200 GeV/c

Experiment	Interaction ($p_{lab}, GeV/c$)	$B_{\psi'}\sigma_{\psi'}/B_{J/\psi}\sigma_{J/\psi}$ (%)	correction	$B_{\psi'}\sigma_{\psi'}/B_{J/\psi}\sigma_{J/\psi}$ (%) after correction
R702	$p-p(\sqrt{s}=63)$	1.9±0.7	0.811±0.013	1.54±0.60
E705	$p(300)-Li$	1.88±0.31	0.945±0.004	1.78±0.30
E288	$p(400)-Be$	1.7±0.5	0.914±0.006	1.55±0.47
E444	$p(225)-C$	1.6±0.9	0.982±0.001	1.57±0.88
NA51	$p(450)-H_2$	1.97±0.06	0.902±0.006	1.78±0.07
NA51	$p(450)-D_2$	2.03±0.06	0.902±0.006	1.83±0.07
NA38	$p(450)-C$	2.07±0.26	0.902±0.006	1.87±0.25
NA38	$p(450)-Al$	1.24±0.32	0.902±0.006	1.12±0.30
NA38	$p(450)-Cu$	1.76±0.15	0.902±0.006	1.59±0.15
NA38	$p(200)-W$	1.77±0.11	1	1.77±0.11
NA38	$p(450)-W$	1.70±0.18	0.902±0.006	1.53±0.17
NA38	$p(200)-U$	2.01±0.46	1	2.01±0.46

Figure 3 shows the trends of the ratio $B_{\psi'}\sigma_{\psi'}/B_{J/\psi}\sigma_{J/\psi}$ as a function of the target mass number A for all our p-A systems at (or rescaled to) 200 GeV/c, together with the other experiment's results. A linear fit gives a slope of $-0.048\% \pm 0.055\%$, with $\chi^2/ndf = 0.9$, which is consistent with no evolution against A. Thus, the ratio has a mean value of $1.76\% \pm 0.04\%$.

4.2. Study of S-U interactions

Our report refers to the last data taking period with sulphur beam (1992). An average with the previous $\psi'/J/\psi$ cross section values, relative to the 1987-1991 periods (40% of NA38 final statistics), is performed.

The $cos\ \theta^*$ kinematical domain is again $-0.5 < cos\ \theta^* < 0.5$ but, to ensure the same muon paths in all absorbers, the S-U analysis is confined to the rapidity domain of $-0.5 < y_{cm} < 0.5$. Events were split in four equipopulated E_T^o regions. Table 3 shows the number of ψ', J/ψ and signal events, for $M_{\mu\mu} \geq 2.0\ GeV/c^2$ for the analysis of S-U interactions.

Table 3
Number of events in S-U collisions, 1992 period

E_T^o regions	$N_{\mu\mu}^{signal}$ $M_{\mu\mu} \geq 2.0\ GeV/c^2$	$N^{J/\psi}$	$N^{\psi'}$
1^{st}	22396	18233	252
2^{nd}	36697	29570	329
3^{rd}	40723	32322	226
4^{th}	40795	31983	220

To extract cross sections, ψ' and J/ψ are again corrected for acceptance. In order to put together our systems, that is, all p-A and S-U results, we also used the variable L, the particle mean path in the target nucleus, which is, as E_T^o, a measure of the collision centrality.

Table 4 shows the trends of the ratio $B_{\psi'}\sigma_{\psi'}/B_{J/\psi}\sigma_{J/\psi}$ as a function E_T^o (and L) for the whole NA38 statistics, that is, putting together the results of the 1987, 90, 91 and 92 data taking periods.

Table 4
Ratio $B_{\psi'}\sigma_{\psi'}/B_{J/\psi}\sigma_{J/\psi}$ as a function of E_T^o and L for S-U collisions

E_T^o region (GeV)	$<E_T^o>$ (GeV)	$L(fm)$	$B_{\psi'}\sigma_{\psi'}/B_{J/\psi}\sigma_{J/\psi}$
13 - 34	23.7	6.7	1.11 ± 0.12
34 - 56	44.6	7.8	0.97 ± 0.10
56 - 75	65.1	9.0	0.68 ± 0.09
75 -110	86.9	10.2	0.62 ± 0.09
$\geq$13	55.7	8.5	0.83 ± 0.06

In Figure 4 we show the evolution of the ratio $B_{\psi'}\sigma_{\psi'}/B_{J/\psi}\sigma_{J/\psi}$ for all p-A and S-U results, as a function of L. One clearly sees that, while in p-A data the ratio is flat against L, i.e., ψ' has the same behaviour as J/ψ, S-U results show a clear departure: ψ' becomes more and more suppressed with respect to J/ψ as L increases. Thus, ψ' behaviour, as compared to J/ψ, is different when passing from p-A interactions to S-U collisions. Nevertheless, if we perform a global linear fit to our data points we obtain a slope of -0.116 ± 0.008 with a bad χ^2/ndf: 3.4 .

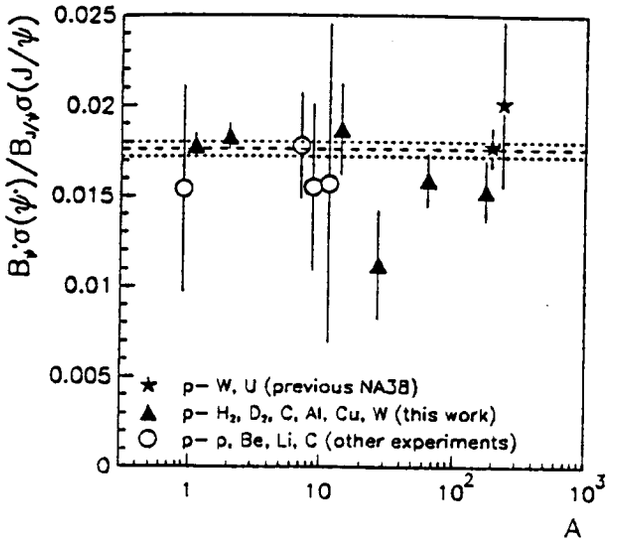

Figure 3. Ratio $B_{\psi'}\sigma_{\psi'}/B_{J/\psi}\sigma_{J/\psi}$ as a function of A for p-A interactions. Dashed and dotted lines represent p-A mean value and error.

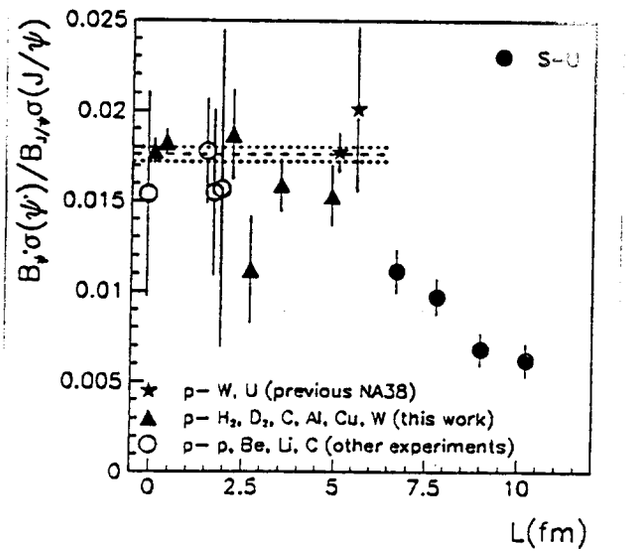

Figure 4. Ratio $B_{\psi'}\sigma_{\psi'}/B_{J/\psi}\sigma_{J/\psi}$ as a function of L for p-A and S-U interactions. Dashed and dotted lines represent p-A mean value and error.

5. STUDY OF DIRECT PHOTON EMISSION

5.1. Principle of the method

Our aim is to investigate the γ/π^o yields correlated with the dimuon mass $M_{\mu\mu}$, namely with J/ψ and ϕ, using our S-U data. The study is performed in the pseudorapidity range of $1.7 < \eta_{lab} < 4.2$.

The electromagnetic calorimeter measures E_T^o, which is mainly due to photons, either originating from hadron decays (essentially π^o) or, very rarely, directly produced. One has, thus, $E_T^o \simeq E_T^{\pi^o} + E_T^\gamma$.

The target cylindrical hodoscope measures n_{ch}, which gives the number of charged particles (mostly minimum ionizing pions), i.e., $n_{ch} \simeq 2 \cdot n_{\pi^o}$.

Assuming thermal γ, $\bar{P}_T^\gamma = \bar{P}_T^\pi$, one derives the γ to π^o ratio:

$$\frac{n_\gamma}{n_{\pi^o}} \simeq \frac{(E_T^o/\bar{P}_T - n_{ch}/2)}{n_{ch}/2} \quad ,$$

with small statistical errors, but larger systematic errors ($\sim 20\%$) than the expected effect ($\sim 1\%$).

For this reason we prefer to study ratio differences, e.g. $n_\gamma/n_{\pi^o}(\phi) - n_\gamma/n_{\pi^o}(J/\psi)$, which are meaningful as systematic errors largely cancel.

5.2. Data correction

Assuming multiparticle production limited to pions and direct gammas, the calorimeter yields $E_T^{o,meas} = \bar{P}_T^\pi(n_{\pi^o} + f_{ch}n_{\pi^\pm}) + \bar{P}_T^\gamma n_\gamma$, where $f_{ch}n_{\pi^\pm}$ weights the contribution due to charged pions, and the target hodoscope yields a signal proportional to a multiplicity,

$n_{ch} = [n_{\pi^\pm} + f_\gamma(2n_{\pi^o} + n_\gamma)]$, with f_γ being the fraction of additional charges due to γ induced electron pair creation in subtargets. A Monte-Carlo is used to extract these f quantities.

In order to have a perfectly linear correlation between the two variables E_T^o and E_T^{ch}, which are derived from the previous measured quantities, we perform some data corrections, such as equalizing $E_T^{o,meas}$ and n_{ch} resolutions and normalizing the n_{ch} mean on the one of $2 \cdot E_T^{o,meas}$. These correction factors are established on the whole sample of dimuon data (opposite and like-sign) and over the mass range of $0.5 \leq M_{\mu\mu} \leq 3.5\ GeV/c^2$ (38K events). One obtains:

$E_T^o = \overline{P}_T \cdot (n_{\pi^o} + 0.66 n_\gamma^{dir})$

$E_T^{ch} = \overline{P}_T \cdot (n_{\pi^\pm} + 0.22 \cdot n_\gamma^{dir}) = \overline{P}_T \cdot (2 \cdot n_{\pi^o} + 0.22 \cdot n_\gamma^{dir})$.

Figure 5 shows such a correlation between these two derived variables.

5.3. Results

Now, defining the averaged transverse energy $E_T^{av} = 1/3 \cdot (E_T^o + E_T^{ch})$, we can express the relative excess of neutral transverse energy by: $\Delta = (E_T^o - 0.5 \cdot E_T^{ch})/E_T^{av}$, from which we extract: $\frac{n_\gamma}{n_{\pi^o}} \equiv \frac{\gamma}{\pi^o} = 1.81 \cdot \Delta$.

In order to minimize systematic errors, we study ratio differences $\Delta^{S-J/\psi} \equiv \Delta^S - \Delta^{J/\psi}$ or, in another way, $< \frac{\gamma}{\pi^o} >^S - < \frac{\gamma}{\pi^o} >^{J/\psi} = 1.81 \cdot \Delta^{S-J/\psi}$. S stands for each of the dimuon mass regions that are compared to the J/ψ one: $\rho + \omega$, ϕ and continuum (defined as $1.25 < M_{\mu\mu} < 2.70\ GeV/c^2$). The fraction of main signal in each mass region is: $\rho + \omega$: 80%, ϕ: 78%, continuum: 98% and J/ψ: 96%. Figures 6, 7 and 8 show such differences for S-U collisions (with $\Delta^{S-J/\psi}$ on the left vertical scale and $< \frac{\gamma}{\pi^o} >^{S-J/\psi}$ on the right one) as a function of E_T^{av}. No direct photon enhancement correlated with any particular mass region, as compared to the J/ψ one, is found. The broken lines concern the $< \gamma/\pi^o >$ variable and they indicate a 3between low mass channels and the J/ψ .

In Table 5 are shown integrated values for two most central E_T^{av} bins representing 80% and 35% most central dimuon trigger events. The fraction of corresponding minimum bias events are estimated to be 25% and 8%, respectively.

Table 5
γ/π^o differences for near head-on S-U collisions

centrality	$\Delta^{\rho-J/\psi}$	$\Delta^{\phi-J/\psi}$	$\Delta^{Cont.-J/\psi}$
25%	0.6 ± 0.7	0.4 ± 0.7	0.0 ± 1.3
8%	1.2 ± 1.0	-0.4 ± 1.0	0.8 ± 1.8

We notice that no significant differences within $\pm 2\%$ $(90 - 95\%\ CL)$ on the γ/π^o ratio between the $\rho + \omega$, ϕ, or continuum channels and the J/ψ one are seen in central S-U interactions.

These result holds as far as all channels (J/ψ, ϕ, ...) have the same hadronic structure. A complete simulation using a more realistic picture of emitted particles and strangeness enhancement, rather than our only pion assumptions, will be undertaken to precise these results.

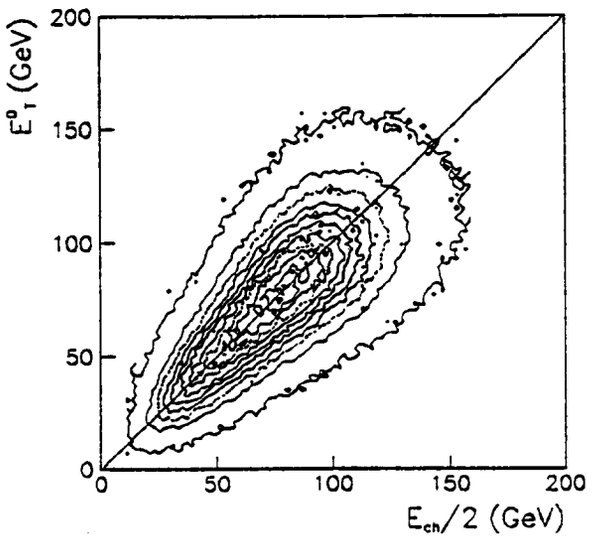

Figure 5. Correlation between neutral and charged multiplicities. Contour lines decrease by steps of 10%, the external one representing 1% of the maximum.

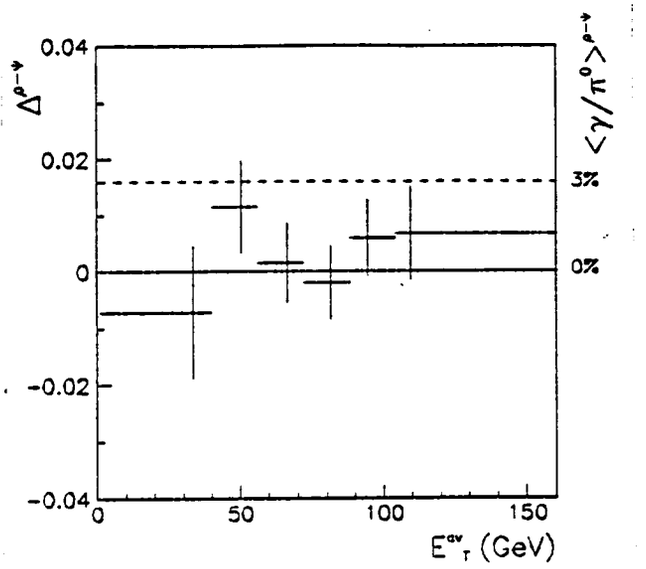

Figure 6. Neutral relative mean excess between $\rho + \omega$ and J/ψ region.

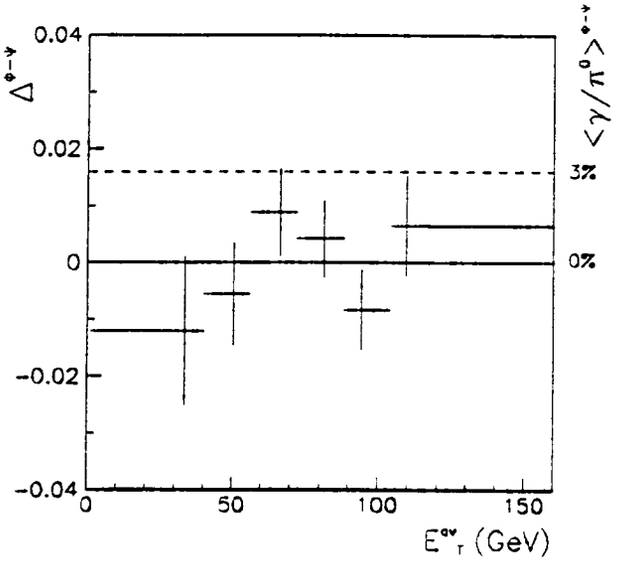

Figure 7. Neutral relative mean excess between ϕ and J/ψ region.

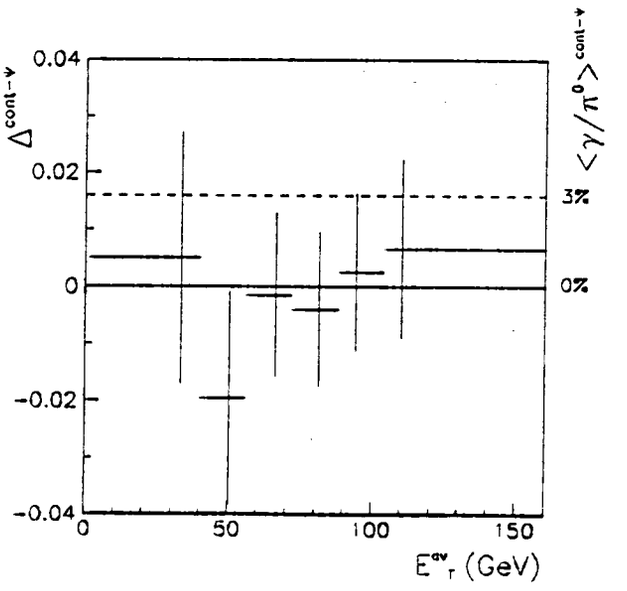

Figure 8. Neutral relative mean excess between continuum and J/ψ region.

6. CONCLUSIONS

In p-A interactions the $B_{\psi'}\sigma_{\psi'}/B_{J/\psi}\sigma_{J/\psi}$ ratio remains constant going from p-p and p-d collisions to p-W and p-U ones, with a mean value of 1.76% ± 0.04%. In the S-U interactions the $B_{\psi'}\sigma_{\psi'}/B_{J/\psi}\sigma_{J/\psi}$ ratio has value of 0.83% ± 0.06% when integrated in E_T^o, and it decreases by almost a factor of two as centrality increases. These results imply that, while ψ' and J/ψ behave in the same way in p-A, ψ' is more suppressed than J/ψ in S-U collisions.

Concerning direct photon production, our results, if confirmed, shed some doubts on the picture of stochastically occuring QGP, where ϕ events tag QGP reactions while J/ψ ones survive when QGP is not formed.

REFERENCES

1. S. Gupta and H. Satz, Phys. Lett. B283 (1992) 439.
2. NA38 Collab., C. Baglin et al., Phys. Lett. B255 (1991) 459.
3. NA38 Collab., C. Baglin et al., Phys. Lett. B272 (1991)) 449;
   R. Ferreira, QM'91, Nucl. Phys. A544 (1992) 497c.
4. NA38 Collab., C. Baglin et al., Phys. Lett. B220 (1989) 471.
5. NA51 Collab., A. Baldit et al., Phys Lett 332B (1994) 244.
6. M. Glück, E. Reya, A. Vogt, Z. Phys. C53 (1992) 127.
7. C. Gerschel and J. Hüfner, Z. Phys. C56 (1992) 171.
8. NA38 Collab., M.C. Abreu et al., Nucl. Phys. A566 (1994) 77c;
   NA38 Collab., M.C. Abreu et al., Nucl. Phys. A566 (1994) 371c.
9. R702 Collab., A.G. Clark et al., Nucl. Phys. B142 (1978) 29;
   E705 Collab., L. Antoniazzi et al., Phys. Rev. D46 (1992) 4828;
   E288 Collab., H.D. Snyder et al., Phys. Rev. Lett. 36 (1976) 1415;
   E444 Collab., K.J. Anderson et al., Phys. Rev. Lett. 42 (1979) 944.